Applied Catalysis B: Environmental 259 (2019) 118038

Contents lists available at ScienceDirect

Applied Catalysis B: Environmental

journal homepage: www.elsevier.com/locate/apcatb

Anthraquinones as photoredox active ligands of TiO_2 for selective aerobic oxidation of organic sulfides

Huimin Hao[a], Xia Li[a], Xianjun Lang[a,b,*]

[a] Sauvage Center for Molecular Sciences, College of Chemistry and Molecular Sciences, Wuhan University, Wuhan 430072, China
[b] Key Laboratory of Advanced Energy Materials Chemistry (Ministry of Education), Nankai University, Tianjin 300071, China

ARTICLE INFO

Keywords:
Anthraquinones
Photoredox active ligands
Selective oxidation
Organic sulfides
Anatase TiO2

ABSTRACT

Anthraquinones (AQs) are well-known for their excellent redox properties. In this contribution, AQs were designated as a photoredox active ligand of TiO_2 for selective aerobic oxidation of organic sulfides. Importantly, we have found that there is an interrelation between the structural nuances of AQs and the conversions of sulfides. Particularly, with 2 mol% of (2,2,6,6-tetramethylpiperidin-1-yl)oxyl (TEMPO) as the redox mediator, organic sulfides can be selectively oxidized into sulfoxides with aerial O_2 by 1,2-dihydroxyanthraquinone (1,2-DHA) acting a photoredox active ligand of anatase TiO_2 under visible light illumination. This work highlights the potential of designing photoredox active ligand of metal oxide semiconductors to construct visible-light-induced selective aerobic oxidation reactions.

1. Introduction

Anthraquinones (AQs) are well-recognized for their exceptional redox properties. One notable demonstration of the redox resilience of AQs is the large industrial scale application of 2-ethylanthraquinone (EAQ) for the production of hydrogen peroxide (H_2O_2) from hydrogen (H_2) and oxygen (O_2). AQs have been applied into industry as the catalyst for the production of hydrogen peroxide (H_2O_2) with a long history and the process is constantly improving [1]. In the industrial anthraquinone process, firstly, the EAQ will be reduced into 2-ethylanthrahydroquinone ($EAQH_2$) by H_2; secondly, the $EAQH_2$ goes to reduce O_2 into H_2O_2 automatically; simultaneously, the $EAQH_2$ will return back to EAQ [2]. Inspired by this challenging reaction, AQs in principle could be considered as an efficient oxidation catalyst using O_2 as the terminal oxidant. In addition, the redox property of AQs also leads to a variety of biological activities, such as anti-cancer effect, anti-inflammatory, antinociceptive activities and so on [3,4].

Apart from the above redox properties, AQs are also the building block for one group of the most abundant dyes, second only to azo dyes. As organic textile dyes, AQs were under significant developments during the past decades [5]. This particular application in part depends on the wide range of colors of AQs, indicative of the potential of this type of molecules in absorbing a wide range of visible light. Plus, this is also a manifestation of good binding characteristic of AQ dyes towards textile fibers. Visible light photocatalysis can realize the selective aerobic oxidation of organic compounds in an economical and clean way [6,7], and the types of photocatalysts varies from inorganic semiconductors to emerging materials [8–10]. With the combined redox and light-harvesting properties, one could hypothesize AQs can be visible light photocatalysts for aerobic oxidative transformations. To our surprise, AQs received scant attention in this application [11]. Recently, 1,8-dihydroxyanthraquinone (1,8-DHA) has been employed for the visible-light-induced reduction of aryl halides [12]. More importantly, AQs has been proven as a potential candidate for the photocatalytic generation of H_2O_2 [13,14]. However, the highest occupied molecular orbital (HOMO) position of AQs is not favorable to smoothly reduce O_2. Therefore, relying on AQs as the photocatalysts, the selective aerobic oxidation of organic compounds cannot occur successfully under visible light illumination. Because the HOMO level might make it suitable for other reaction [15] rather than selective aerobic oxidation reactions. Most of the literature reports centered on the photochemical degradation of AQ dyes mediated by semiconductor surfaces [16–19]. From a different perspective, one can conclude that, by interaction with semiconductors, AQs have been transformed for the favorable activation of O_2. To this end, the adsorption and reactions of O_2 on anatase TiO_2 has garnered much attention [20,21]. Naturally, it is wise choice to select anatase TiO_2 to aid in AQs for the activation of O_2 to $O_2^{\cdot -}$ (-0.33 V vs NHE) under visible light illumination, due to its suitable conduction band potential (-0.50 V vs NHE).

TiO_2 has been applied in photocatalysis for a long history, but the

* Corresponding author at: Sauvage Center for Molecular Sciences, College of Chemistry and Molecular Sciences, Wuhan University, Wuhan 430072, China.
E-mail address: xianjunlang@whu.edu.cn (X. Lang).

https://doi.org/10.1016/j.apcatb.2019.118038
Received 4 June 2019; Received in revised form 29 July 2019; Accepted 31 July 2019
Available online 01 August 2019
0926-3373/

lack of visible light absorption has hampered its application severely because of the wide band gap [22,23]. It is noteworthy that anatase TiO_2, a well-known semiconductor photocatalyst, can be introduced to aid in this critical step, providing conduction band to mediate electron transfers from donors to acceptors like O_2 [24]. Our research group discovered that xanthene dyes such as eosin Y or 5(6)-carboxyfluorescein were anchored onto anatase TiO_2 for photocatalytic aerobic oxidation of alcohols [25,26]. Nevertheless, alizarin red S (ARS), one of the most representative AQ dye, turns out to be the most outstanding one for decorating anatase TiO_2 for visible light photocatalytic aerobic oxidations. For example, ARS-sensitized TiO_2 has been utilized for the photocatalytic selective aerobic oxidation of alcohols [27–29], amines [30] and sulfides [31,32] under visible light illumination. However, the molecular underpinning of ARS for the unique effectiveness remains elusive in these schemes. To some extent, ARS can be considered as a surface ligand for anatase TiO_2 in constructing an efficient visible light photocatalyst. Thus, we adopted a reverse molecular engineering strategy by the analysis the molecular structures of ARS and kept the main scaffold unchanged throughout the investigation of a series of AQs. By altering the substituting groups in AQ to figure out the major molecular design in contributing most photoredox active AQ ligands in the selective oxidation of organic compounds.

To our knowledge, sulfoxides are pivotal chemical and pharmaceutical intermediates [33]. As an atom-economic route for the direct synthesis of sulfoxides, the selective aerobic oxidation of organic sulfides into sulfoxides is a significant reaction [34,35]. However, this procedure often suffers from the problem of over-oxidation and low selectivity. To date, many efforts have been implemented to try to overcome the drawback [36–38]. By controlling the crystal structure of photocatalyst TiO_2, this problem also has been alleviated to some extent [39]. As a member of AQs, ARS-TiO_2 assembly has been confirmed to be an elegant photocatalyst for the selective oxidation of sulfides under visible light illumination [31]. Inspired by the molecular structure of ARS, we are looking forward to create more effective photocatalysts from the view of molecular design and explore the relationship of photocatalytic activities and structures of photoredox active ligands.

Herein, we chose a series of AQs as photoredox active ligands for the surface of TiO_2, forming the photocatalysts for the selective aerobic oxidation of organic sulfides. As the photoredox active ligands, AQ molecules match with TiO_2 ingeniously, composing the desirable photocatalysts with type II of electronic excitation mode under illumination. Inspired by the molecular structure of ARS, these AQ ligands focus on AQ and its hydroxyl-substituted derivatives. In this protocol, the home-made anatase TiO_2 makes great improvement in the selectivities. Thus we selected the home-made anatase TiO_2 for our research presented here. With 2 mol% TEMPO as the redox mediator, the selective aerobic oxidation of organic sulfides, supported by 1,2-DHA as photoredox active ligand for the anatase TiO_2, can attain high conversion and selectivity under 520 nm green LED illumination. Benefited from its unique molecular structure, 1,2-DHA can be an ideal molecule to bridge the gap between dye-TiO_2 assembly [40] and TiO_2 surface complexes [41] visible light photocatalysts. Besides, it was evidenced that bidentate chelating binding was necessary for the better photocatalytic process.

2. Experimental section

2.1. Reagents and solvents

The home-made anatase TiO_2 was prepared from the hydrolysis of titanium tetraisopropoxide following previous details [39]. Other reagents were supplied by the companies such as Sigma-Aldrich, Alfa Aesar and TCI, J&K Scientific, etc. The solvents were supplied by Merck, Fischer Scientific and Sinopharm Chemical Reagent Co. Ltd., China. Methanol-D_4 was purchased from Cambridge Isotope Laboratories, Inc. Apart from the home-made anatase TiO_2, all the other reagents and solvents were obtained from commercial suppliers and used without further purification.

2.2. The typical procedure for photocatalytic test

At first, put 50 mg of TiO_2, 1×10^{-3} mmol of 1,2-DHA, 0.006 mmol of TEMPO and 0.3 mmol of sulfide into a 10 mL Pyrex reactor containing 1 mL of CH_3OH as the solvent. After 5 min of ultrasonication, the mixture were stirred for 30 min under the dark condition to achieve adsorption-desorption equilibrium. Next, the rubber septum of Pyrex reactor was punched a hole to connect with aerial O_2. Afterwards, the reactor was magnetically stirred at 1500 rpm and illuminated by the 520 nm green LED simultaneously. In the end, the photocatalyst nanoparticles were separated from the reaction mixture by centrifugation. And the reaction products were analyzed by gas chromatography equipped with a flame ionization detector (GC-FID) using chlorobenzene as the internal standard. The structures of products were confirmed by comparison with the retention time with authentic samples by GC-FID and further confirmed by gas chromatography-mass spectrometry (GC–MS). The instrumental conditions and analysis details were offered in the supporting information.

3. Results and discussion

To find the best AQ ligand for the selective oxidation of thioanisole, we chose the listed six AQ molecules (Fig. 1) for comparison. These AQs have similar skeleton structure and the nuances are composed by the related fragments of ARS, which play essential roles in the formations and activities of complexes photocatalysts. Therefore, the nuances of these different complexes formed from AQs and TiO_2 on the visible-

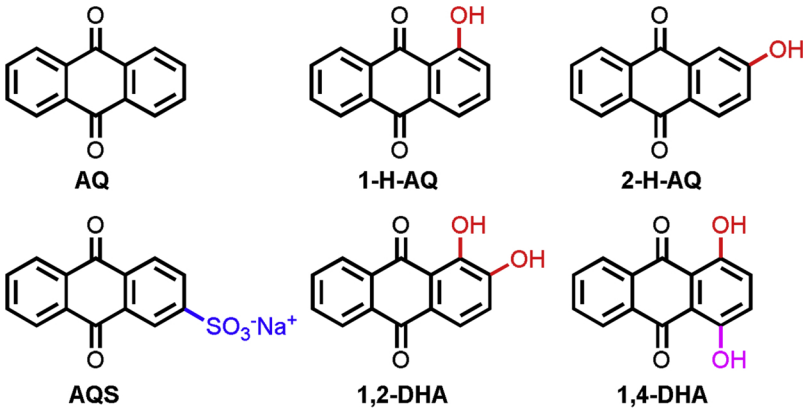

Fig. 1. Different AQs as photoredox active surface ligands for anatase TiO_2.

Table 1
The influence of AQs as photoredox active ligands of TiO_2 on selective aerobic oxidation of thioanisole[a].

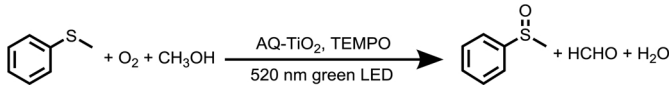

Entry	AQ ligand	Conv.[%][b]	Sel.[%][b]
1	AQ	2	99
2	1-H-AQ	16	98
3	2-H-AQ	63	95
4	AQS	2	99
5	1,2-DHA	75	94
6	1,4-DHA	3	99

[a] Reaction conditions: thioanisole (0.3 mmol), AQ ligand (1×10^{-3} mmol), TiO_2 (50 mg), TEMPO (0.006 mmol), aerial O_2, 520 nm green LED illumination (3 W × 4), CH_3OH (1 mL), 1 h.
[b] Determined by GC-FID using chlorobenzene as the internal standard, conversion of thioanisole, selectivity of methyl phenyl sulfoxide.

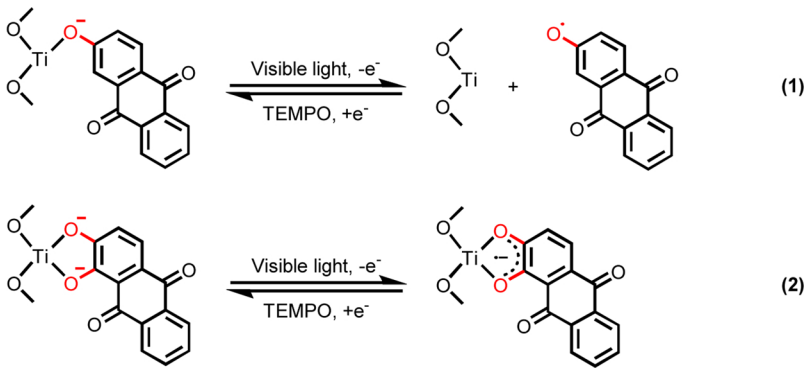

Scheme 1. The two different chelating bindings of hydroxyl-substituted AQs on the surface of anatase TiO_2.

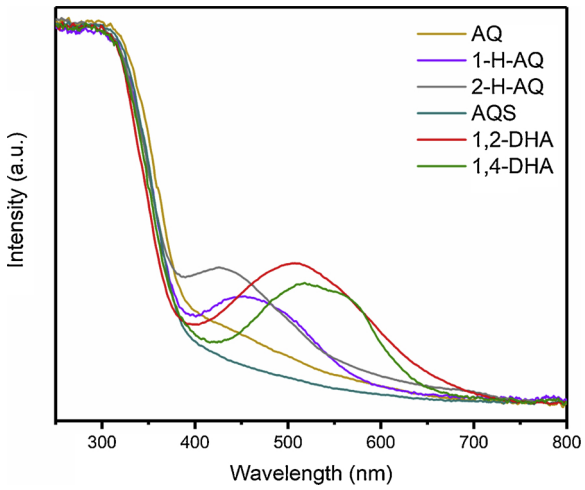

Fig. 2. The diffuse reflectance UV–vis spectroscopy of different AQs as ligands for anatase TiO_2 surface.

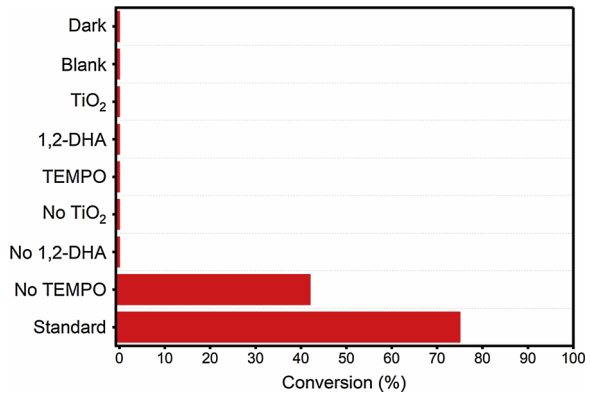

Fig. 3. Control experiments for the selective aerobic oxidation of thioanisole with 1,2-DHA as a photoredox active ligand of TiO_2. Standard reaction conditions: thioanisole (0.3 mmol), TiO_2 (50 mg), 1,2-DHA (1×10^{-3} mmol), TEMPO (0.006 mmol), CH_3OH (1 mL), 520 nm green LED illumination (3 W × 4), aerial O_2, 1 h. Conversions of thioanisole were determined by GC-FID using chlorobenzene as the internal standard.

light-induced selective aerobic oxidation of sulfides were checked respectively (Table 1). Under the same reaction conditions, AQ and sodium anthraquinone-2-sulfonate (AQS) almost cannot promote the oxidation of thioanisole (entries 1 and 4, Table 1). In contrast, the presence of hydroxyl groups increases the photocatalytic activity (entries 2,3 and 5, Table 1), which was attributed to the more competent and stabilized binding way of hydroxyl groups from substituted AQs and TiO_2 surface (Scheme 1). Moreover, it is demonstrated that the relative position of hydroxyl group will affect the binding process by the completely different conversions between 1,2-DHA and 1,4-dihydroxyanthraquinone (1,4-DHA). As the photoredox active ligand, 1,2-DHA has the highest promotion for the oxidation of sulfide under 520 nm green LED illumination (entry 5, Table 1). Indeed, the 1,2-DHA molecule fixed on the identical Ti site of the TiO_2 successfully through the bi-dentate chelating binding pattern (Eqn (2)) rather than the mono-dentate chelating bindings (Eqn (1)), and this binding way is advantageous to the migration of excited electrons from the bounded dyes to the conduction band of TiO_2 [42]. However, the two hydroxyl groups of 1,4-DHA do not locate in the appropriate sites, so that its photocatalytic activity are largely unsatisfactory (entry 6, Table 1).

In view of the PXRD patterns of our different photocatalysts (Fig. S1), we can conclude that the loading of AQs on the TiO_2 does not change the crystal structure of TiO_2. From the specific surface area (Table S1), we predict that the loading of 1,2-DHA on the TiO_2 is the

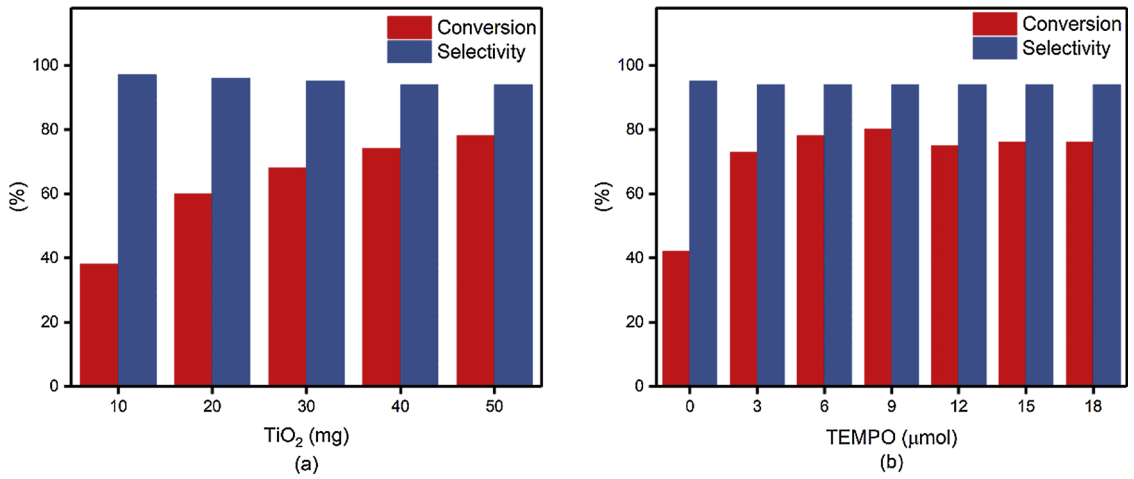

Fig. 4. The influence of the amount of (a) TiO_2 and (b) TEMPO on the selective aerobic oxidation of thioanisole with 1,2-DHA as a photoredox active ligand of TiO_2. Reaction conditions: thioanisole (0.3 mmol), 1,2-DHA (1×10^{-3} mmol), CH_3OH (1 mL), 520 nm green LED illumination (3 W × 4), 1h. (a) TEMPO (0.006 mmol), (b) TiO_2 (50 mg). Conversions of thioanisole and selectivities of methyl phenyl sulfoxide were determined by GC-FID using chlorobenzene as the internal standard.

Table 2
Quenching experiments to determine the ROS for the selective aerobic oxidation of thioanisole with 1,2-DHA as a photoredox active ligand of TiO_2[a].

Entry	Quencher (equiv.)	Role	Conv.[%][b]	Sel.[%][b]
1	*p*-BQ (0.2)	$O_2^{\cdot -}$ scavenger	4	99
2	$AgNO_3$ (1)	electrons scavenger	0	–
3	DABCO (0.1)	singlet oxygen scavenger	72	92
4	N_2 (-)	O_2 replacement	0	–

[a] Reaction conditions: thioanisole (0.3 mmol), TiO_2 (50 mg), 1,2-DHA (1×10^{-3} mmol), TEMPO (0.006 mmol), CH_3OH (1 mL), 520 nm green LED illumination (3 W × 4), aerial O_2, 1 h.
[b] Determined by GC-FID using chlorobenzene as the internal standard, conversion of thioanisole, selectivity of methyl phenyl sulfoxide.

Table 3
The influence of initial O_2 pressure on the selective aerobic oxidation of thioanisole with 1,2-DHA as a photoredox active ligand of TiO_2[a].

Entry	Initial O_2 pressure [atm]	Conv.[%][b]	Sel.[%][b]
1	0.2	75	94
2	0.5	80	94
3	1.0	86	93
4	1.5	88	92
5	2.0	89	91
6	2.5	90	91

[a] Reaction conditions: thioanisole (0.3 mmol), TiO_2 (50 mg), 1,2-DHA (1×10^{-3} mmol), TEMPO (0.006 mmol), CH_3OH (1 mL), 520 nm green LED illumination (3 W × 4), 1 h.
[b] Determined by GC-FID using chlorobenzene as the internal standard, conversion of thioanisole, selectivity of methyl phenyl sulfoxide.

largest and the most stable one according to the minimal surface area after binding. As for the diffuse reflectance UV–vis spectroscopy (Fig. 2), the difference between 1,2-DHA and AQ, 1-hydroxyanthraquinone (1-H-AQ), 2-hydroxyanthraquinone (2-H-AQ), AQS is rather obvious, and the difference between 1,2-DHA and 1,4-DHA is relatively smaller. Hence, 1,2-DHA stands out with higher photocatalytic activity, which is caused by not only the different absorbance, but also the unique binding structure (Scheme 1). Then, we explored the effects of different wavelengths of LEDs on the reaction (Table S2). Taking the background blue light absorption of TiO_2 into consideration, 520 nm green LED was chosen for the follow-up experiments. Different types of TiO_2 have different photocatalytic performance (Table S3). The home-made anatase TiO_2 was picked out owing to its better action in

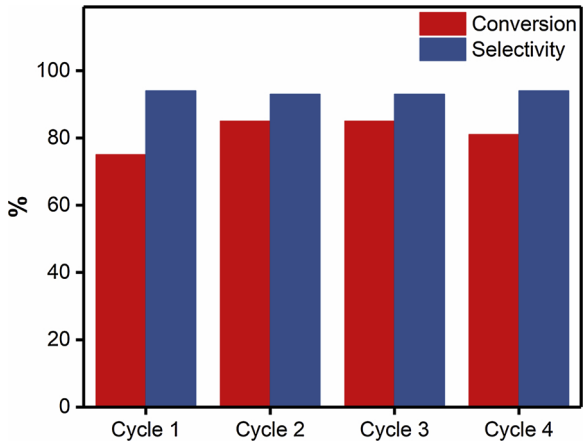

Fig. 5. The recycling test of 1,2-DHA as a photoredox active ligand of TiO_2 on the selective aerobic oxidation of thioanisole.

improving the selectivity of sulfoxide.

To gain insight into the function of each component in the system, control experiments have been executed and the results were expressed in Fig. 3. So TiO_2, 1,2-DHA and visible light source are required as the supporting, photoredox active ligand and stimulating motivation, respectively. Lacking in any one of the three, the selective aerobic oxidation cannot occur. In particular, without TiO_2, the electron transfer from 1,2-DHA to O_2 cannot happen without the mediation of semiconductor conduction band, causing the oxidation to stop (No TiO_2, Fig. 3). The existence of 1,2-DHA molecule dominates the visible light absorption of photocatalyst. As the redox mediator, TEMPO accelerates the oxidation significantly, playing an important role in the photocatalytic procedure. And the more detailed impacts of TEMPO will be discussed later (Fig. 4b).

The reactive oxygen species (ROS) dominate the overall selective aerobic oxidation of organic sulfide, which was confirmed by the quenching experiments (Table 2). We adopted a strategy of capturing the possible ROS separately. When different quenchers were introduced into the photocatalytic process, the reactions showed varying degrees of drop. As the famous $O_2^{\cdot -}$ scavenger, *p*-benzoquinone (*p*-BQ) was added into our photocatalytic system. The sharp decline of conversion indicates that $O_2^{\cdot -}$ is the main ROS for our photocatalytic reaction (entry 1, Table 2). $AgNO_3$ ceased the reaction thoroughly by arresting the electrons (entry 2, Table 2), which suggested the reaction followed the electron transfer mechanism indirectly. In contrast, 1,4-diazabicyclo

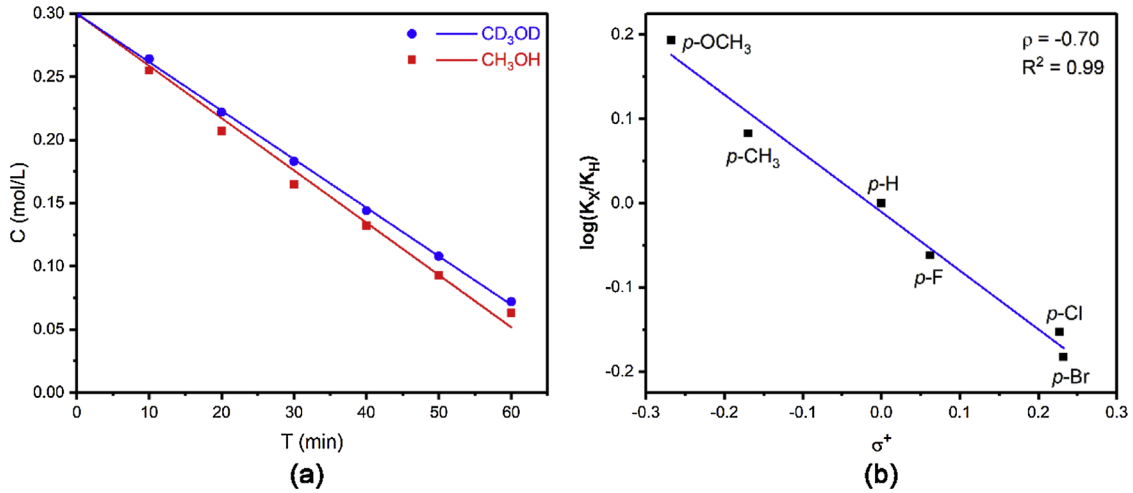

Fig. 6. (a) The reaction kinetic studies of the selective aerobic oxidation of thioanisole with 1,2-DHA as a photoredox active ligand of TiO_2 in CD_3OD and CH_3OH; (b) The Hammett plot for the selective aerobic oxidation of *para*-substituted thioanisoles with 1,2-DHA as a photoredox active ligand of TiO_2.

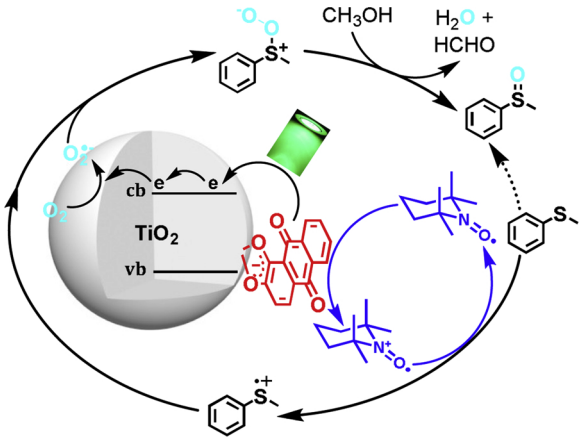

Fig. 7. The proposed mechanism for the selective aerobic oxidation of organic sulfide with 1,2-DHA as a photoredox active ligand of TiO_2.

[2.2.2]octane (DABCO) does not have an evident impact on the selective aerobic oxidation of thioanisole (entry 3, Table 2). Therefore, singlet oxygen is not the major ROS. As we expected, the photocatalytic oxidative procedure cannot occur at all in the absence of O_2 (entry 4, Table 2).

The amount of TiO_2 influences the conversion of thioanisole, rather than the selectivity of product (Fig. 4a). TEMPO, as the co-catalyst, illustrates a sizable enhancement when added into the system (Fig. 4b). It is reasonable that TEMPO boosts the transfer of electrons between the photocatalyst and substrate of thioanisole. However, excessive TEMPO will inhibit the photocatalytic process, because TEMPO might capture the essential ROS, resulting in the stopover of the oxidation. This photocatalytic oxidative reaction becomes faster when the concentrations of thioanisole and photocatalyst grow (Table S4), since thioanisole and photocatalyst have more probability to contact and interact with each other at high concentrations.

As the oxidant, O_2 regulates the whole oxidative process of sulfides and the initial O_2 pressure is a factor that cannot be ignored. Under the listed initial O_2 pressures from 0.2 atm to 2.5 atm, the conversion of thioanisole exhibited certain ascent trend at first, and reached a steady level nearly in the end (Table 3). There is a saturated state of initial O_2 pressures on the selective aerobic oxidation of thioanisole with 1,2-DHA as the photoredox active ligand of TiO_2, but the reaction will not accelerate unlimitedly as the initial O_2 pressure increases.

The photocatalysts have good stability which was proven by the recycling tests (Fig. 5). After four consecutive cycles, the conversion did not undergo clear decrease and the selectivity was also unchanged, illustrating 1,2-DHA-TiO_2 is durable and recyclable as a heterogeneous photocatalyst.

Afterwards, we conducted the reaction kinetic studies of photocatalytic oxidation of thioanisole by 1,2-DHA-TiO_2 in CD_3OD, compared with that in CH_3OH (Fig. 6a). CD_3OD, as a singlet oxygen maintainer, will prolong the lifetime of singlet oxygen. However, the reaction did not go much faster in CD_3OD than CH_3OH, so the singlet oxygen is not the key ROS, which was consistent with the conclusion of control quenching experiments. The Hammett plot was obtained through the kinetic investigation of oxidation of *para*-substituted thioanisoles (Fig. 6b). The value of ρ equals -0.70, a negative value, suggesting that the reaction loses negative charge or builds positive

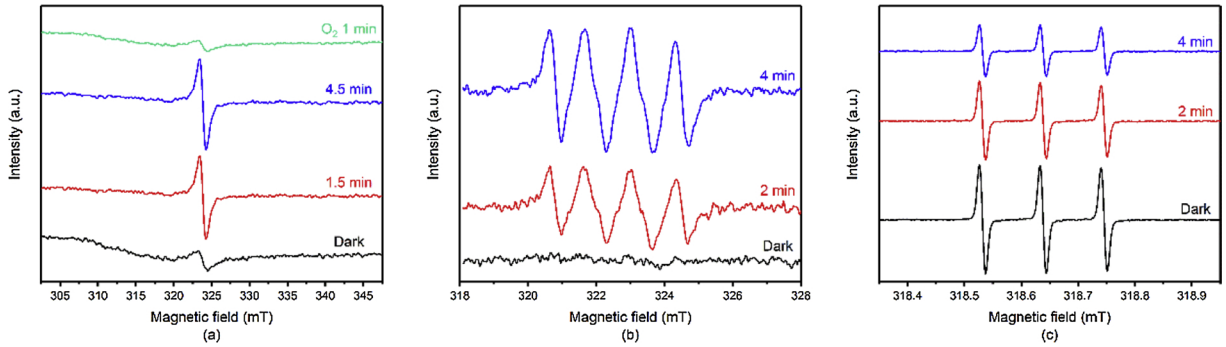

Fig. 8. The EPR spectra recorded during the selective aerobic oxidation of thioanisole with 1,2-DHA as a photoredox active ligand of TiO_2 (a) conduction band electrons of TiO_2; (b) spin trapping of superoxide radicals ($O_2^{\cdot -}$) with DMPO; (c) TEMPO.

Table 4
The selective aerobic oxidation of diverse organic sulfides with 1,2-DHA as a photoredox active ligand of TiO_2[a].

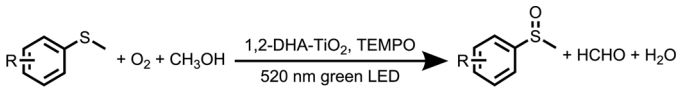

Entry	Substrate	Product	T(h)	Conv.[%][b]	Sel.[%][b]
1			1.3	90	91
2[c]			5	78	92
3	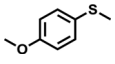	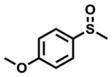	0.9	96	93
4	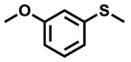	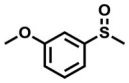	1.5	87	91
5			1.3	93	98
6	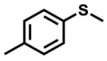	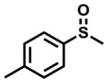	1.1	93	92
7	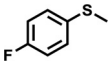	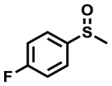	1.3	83	90
8	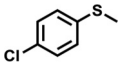	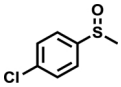	1.7	80	88
9	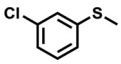	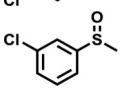	2	70	90
10			2.5	49	98
11	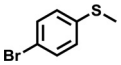	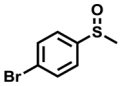	2	86	86
12	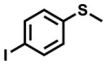	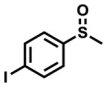	1.7	80	86
13	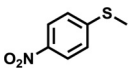	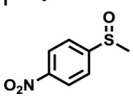	4	31	91
14	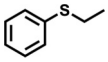	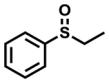	1.5	85	87
15			3	18	91
16	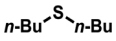	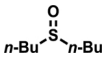	0.6	98	95
17			0.6	96	92

[a] Reaction conditions: sulfide (0.3 mmol), TEMPO (0.006 mmol), TiO_2 (50 mg), 1,2-DHA (1×10^{-3} mmol), CH_3OH (1 mL), 520 nm green LED illumination (3 W × 4), aerial O_2.
[b] Determined by GC-FID using chlorobenzene as the internal standard, conversion of sulfide, selectivity of sulfoxide.
[c] thioanisole (1.5 mmol), TEMPO (0.015 mmol). *n*-Bu, *n*-butyl.

charge most probably and the electron donating groups would facilitate the reaction by resonance stabilization. No measurable amount of H_2O_2 was detected in the photocatalytic system. When 1 equivalent of H_2O_2 was added instead of O_2 as the oxidant, control experiments under dark and illumination conditions indicate there is no impact of it on the photocatalytic oxidation of thioanisole, suggesting that H_2O_2 is not at play in the photocatalytic process.

The proposed mechanism for the selective aerobic oxidation of organic sulfide with 1,2-DHA as a photoredox active ligand of TiO_2 has been illustrated in the Fig. 7. Firstly, the electrons will migrate from

dyes to the conduction band (cb) of TiO_2 under 520 nm green LED illumination. Then the productive e_{cb}^- combined with O_2, establishing $O_2^{\bullet-}$ for the next oxidative procedure as main ROS; 1,2-DHA$^{\bullet+}$ can come back to 1,2-DHA status, coupling with the conversion of TEMPO to 2,2,6,6-tetramethylpiperidine-1-oxoammonium ($TEMPO^+$). The ROS $O_2^{\bullet-}$ intercepts the sulfur centered cations generated from oxidation of sulfide by $TEMPO^+$, proceeding the oxidation of sulfide. During this step, TEMPO will be restored from $TEMPO^+$. With the involvement of protons from solvent CH_3OH, the product sulfoxide were obtained finally. These assumptions were certified again by electron paramagnetic resonance (EPR) spectroscopy (Fig. 8). In the absence of O_2, illumination caused the accumulation of e_{cb}^- of TiO_2 according to the recorded EPR spectra (Fig. 8a). With the subsequent injection of O_2, the signal almost fell back to the status before illumination, suggesting the association of e_{cb}^- and O_2. The signals of $O_2^{\bullet-}$ are recorded evidently with the trapping agent of 5,5-dimethyl-1-pyrroline *N*-oxide (DMPO) in Fig. 8b. When the illumination time prolongs from 0 min to 2 min, 4 min, the signal intensity of TEMPO decreased partly (Fig. 8c), which is ascribed to the generated $TEMPO^+$ is an EPR inactive species and cannot be detected. Overall, the EPR spectra coincide with the proposed mechanism well.

It is affirmed that the oxidation of diverse organic sulfides can proceed with high conversions (Table 4), which is an apropos proof for the catholicity of the 1,2-DHA-TiO_2 photocatalyst. With home-made TiO_2 (see Figure S3 for TEM characterization), the selectivity for methyl phenyl sulfoxide is above 90% at above 90% conversion of thioanisole (entry 1, Table 4) which is higher than that of ST-01 TiO_2 (entry 3, Table S3). Therefore, we measured the densities of surface hydroxyl groups of ST-01 and home-made TiO_2 by thermogravimetric analysis-mass spectrometry (TGA-MS) in line with a reported method [43], which are 5.0 and 8.8 nm^{-2} respectively. The higher density of surface hydroxyl groups of home-made TiO_2 is particularly helpful in improving the selectivity of sulfoxide at high conversion of sulfide. When the amount of thioanisole multiplies five-fold to 1.5 mmol, the reaction can proceed to a conversion of 78% through longer time of 5 h (entry 2, Table 4). The turnover number (TON) is more than 1000, which is a potent example to show the distinct photocatalytic performance of 1,2-DHA-TiO_2. If there is an electron donating group on the benzene ring, the conversions of sulfides get an overall enhancement (entries 3–6, Table 4), attributed to the electronic effect of substituted group. In contrast, the existence of electron withdrawing group has a negative influence on the photocatalytic oxidation of substrates (entries 7–13, Table 4). The steric hindrance of sulfides will have an obvious effect if the methyl of thioanisole are supplanted with a bigger group. For example, the conversion of phenylethyl sulfide displays a slight decline (entry 14, Table 4). When the methyl side of thioanisole was exchanged with a phenyl group, the conversion of sulfide is genuinely undesirable (entry 15, Table 4). The aliphatic sulfides require shorter time (entries 16–17, Table 4) for conversions comparable to that of aromatic sulfides. Totally, the photocatalyst 1,2-DHA-TiO_2 has superior performance on the selective aerobic oxidation of sulfide under 520 nm green LED illumination.

4. Conclusions

Apart from being a considerable group of organic textile dyes, AQs have been widely used in the catalytic redox process. We have discovered the influence of them as photoredox active ligands of anatase TiO_2 on the selective aerobic oxidation of organic sulfides. 1,2-DHA, with the *ortho*-dihydroxyl substituent group, attaches onto TiO_2 through bidentate chelating binding, leading to an outstanding visible light photocatalyst. With 2 mol% TEMPO as co-catalyst, 1,2-DHA-TiO_2 has excellent photocatalytic performance in the selective aerobic oxidation of sulfides into sulfoxides under 520 nm green LED illumination. This is an effective and energy-saving way to realize the formidable organic transformation successfully. Moreover, it offers a favourable model for the visible-light-induced selective organic transformations from the viewpoint of designing photoredox active ligand of metal oxide semiconductors.

Declaration of Competing Interest

The authors declare that they have no known competing financial interests or personal relationships that could have appeared to influence the work reported in this paper.

Acknowledgements

Financial support from the National Natural Science Foundation of China (grant numbers 21773173 and 21503086), the Fundamental Research Funds for the Central Universities (grant number 2042018kf0212), the 111 project (B12015) and the start-up fund of Wuhan University is gratefully acknowledged.

Appendix A. Supplementary data

Supplementary material related to this article can be found, in the online version, at doi:https://doi.org/10.1016/j.apcatb.2019.118038.

References

[1] I.V. Kolesnichenko, P.R. Escamilla, J.A. Michael, V.M. Lynch, D.A. Vanden Bout, E.V. Anslyn, Chem. Commun. 54 (2018) 11204–11207.
[2] Y.X. Cheng, L. Wang, S.X. Lue, Y.Q. Wang, Z.T. Mi, Ind. Eng. Chem. Res. 47 (2008) 7414–7418.
[3] Q. Huang, G. Lu, H.M. Sben, M.C.M. Cbung, C.N. Ong, Med. Res. Rev. 27 (2007) 609–630.
[4] J.G. Park, S.C. Kim, Y.H. Kim, W.S. Yang, Y. Kim, S. Hong, K.H. Kim, B.C. Yoo, S.H. Kim, J.H. Kim, J.Y. Cho, Mediators Inflamm. (2016) 1903849.
[5] A.U. Chaudhari, D. Paul, D. Dhotre, K.M. Kodam, Water Res. 122 (2017) 603–613.
[6] L. Chen, J. Tang, L.N. Song, P. Chen, J. He, C.T. Au, S.F. Yin, Appl. Catal. B: Environ. 242 (2019) 379–388.
[7] P. Chen, L. Chen, Y. Zeng, F. Ding, X. Jiang, N. Liu, C.T. Au, S.F. Yin, Appl. Catal. B: Environ. 234 (2018) 311–317.
[8] J. He, L. Chen, D. Ding, Y.K. Yang, C.T. Au, S.F. Yin, Appl. Catal. B: Environ. 233 (2018) 243–249.
[9] P. Chen, F. Liu, H.Z. Ding, S. Chen, L. Chen, Y.J. Li, C.T. Au, S.F. Yin, Appl. Catal. B: Environ. 252 (2019) 33–40.
[10] L. Xiao, Q. Zhang, P. Chen, L. Chen, F. Ding, J. Tang, Y.J. Li, C.T. Au, S.F. Yin, Appl. Catal. B: Environ. 248 (2019) 380–387.
[11] W.Y. Zhang, J. Gacs, I.W.C.E. Arends, F. Hollmann, ChemCatChem 9 (2017) 3821–3826.
[12] J.I. Bardagi, I. Ghosh, M. Schmalzbauer, T. Ghosh, B. König, Eur. J. Org. Chem. (2018) 34–40.
[13] G.Q. Xu, Y. Liang, F. Chen, J. Mol. Catal. A: Chem. 420 (2016) 66–72.
[14] H.I. Kim, Y. Choi, S. Hu, W. Choi, J.H. Kim, Appl. Catal. B: Environ. 229 (2018) 121–129.
[15] D. Petzold, B. König, Adv. Synth. Catal. 360 (2018) 626–630.
[16] E. Ghazalian, N. Ghasemi, A.R. Amani-Ghadim, J. Mol. Catal. A: Chem. 426 (2017) 257–270.
[17] A. Khataee, B. Kayan, P. Gholami, D. Kalderis, S. Akay, Ultrason. Sonochem. 39 (2017) 120–128.
[18] E. Basturk, M. Karatas, J. Photochem. Photobiol. A: Chem. 299 (2015) 67–72.
[19] A.R. Khataee, M. Zarei, M. Fathinia, M.K. Jafari, Desalination 268 (2011) 126–133.
[20] M. Setvin, U. Aschauer, P. Scheiber, Y.F. Li, W.Y. Hou, M. Schmid, A. Selloni, U. Diebold, Science 341 (2013) 988–991.
[21] Y.F. Li, U. Aschauer, J. Chen, A. Selloni, Acc. Chem. Res. 47 (2014) 3361–3368.
[22] X.Z. Jiang, M. Manawan, T. Feng, R.F. Qian, T. Zhao, G.D. Zhou, F.T. Kong, Q. Wang, S.Y. Dai, J.H. Pan, Catal. Today 300 (2018) 12–17.
[23] H.X. Zong, T. Zhao, G.D. Zhou, R.F. Qian, T. Feng, J.H. Pan, Catal. Today 335 (2019) 252–261.
[24] H. Kisch, Semiconductor Photocatalysis: Principles and Applications, Wiley-VCH, Weinheim, 2014.
[25] Y.C. Zhang, Z. Wang, X.J. Lang, Catal. Sci. Technol. 7 (2017) 4955–4963.
[26] N.N. Wang, J.L. Shi, H.M. Hao, H. Yuan, X.J. Lang, Sustain. Energy Fuel. 3 (2019) 1701–1712.
[27] X. Li, J.L. Shi, H.M. Hao, X.J. Lang, Appl. Catal. B: Environ. 232 (2018) 260–267.
[28] M. Zhang, C.C. Chen, W.H. Ma, J.C. Zhao, Angew. Chem. Int. Ed. 47 (2008) 9730–9733.
[29] V. Jeena, R.S. Robinson, Chem. Commun. 48 (2012) 299–301.
[30] Z. Wang, X.J. Lang, Appl. Catal. B: Environ. 224 (2018) 404–409.
[31] X.J. Lang, J.C. Zhao, X.D. Chen, Angew. Chem. Int. Ed. 55 (2016) 4697–4700.
[32] H.M. Hao, Z. Wang, J.L. Shi, X. Li, X.J. Lang, ChemCatChem 10 (2018) 4545–4554.
[33] A.P. Pulis, D.J. Procter, Angew. Chem. Int. Ed. 55 (2016) 9842–9860.

[34] J.X. Ye, J.Y. Wang, X. Wang, M.D. Zhou, Catal. Commun. 81 (2016) 1–3.
[35] X.R. Zhou, X. Chen, Y.Q. Jin, I.E. Marko, Chem. Asian J. 7 (2012) 2253–2257.
[36] Z.J. Wang, S. Ghasimi, K. Landfester, K.A.I. Zhang, Chem. Commun. 50 (2014) 8177–8180.
[37] Y. Xu, Z.C. Fu, S. Cao, Y. Chen, W.F. Fu, Catal. Sci. Technol. 7 (2017) 587–595.
[38] X. Liang, Z.F. Guo, H.X. Wei, X. Liu, H. Lv, H.Z. Xing, Chem. Commun. 54 (2018) 13002–13005.
[39] H.M. Hao, Z. Wang, J.L. Shi, X. Li, X.J. Lang, ChemCatChem 10 (2018) 4545–4554.
[40] E. Sundin, M. Abrahamsson, Chem. Commun. 54 (2018) 5289–5298.
[41] G. Zhang, G. Kim, W. Choi, Energy Environ. Sci. 7 (2014) 954–966.
[42] Q. Li, Y.K. Che, H.W. Ji, C.C. Chen, H.Y. Zhu, W.H. Ma, J.C. Zhao, Phys. Chem. Chem. Phys. 16 (2014) 6550–6554.
[43] C.Y. Wu, K.J. Tu, J.P. Deng, Y.S. Lo, C.H. Wu, Materials 10 (2017) 566.